HOKKAIDO UNIVERSITY

Title	Selective synthesis of carbon monoxide via formates in reverse water-gas shift reaction over alumina-supported gold catalyst
Author(s)	Ishito, Nobuhiro; Hara, Kenji; Nakajima, Kiyotaka; Fukuoka, Atsushi
Citation	Journal of energy chemistry, 25(2), 306-310 https://doi.org/10.1016/j.jechem.2015.12.005
Issue Date	2016-03
Doc URL	http://hdl.handle.net/2115/68385
Rights	(C) 2015 Science Press and Dalian Institute of Chemical Physics. All rights reserved. © 2016. This manuscript version is made available under the CC-BY-NC-ND 4.0 license http://creativecommons.org/licenses/by-nc-nd/4.0/
Rights(URL)	http://creativecommons.org/licenses/by-nc-nd/4.0/
Type	article (author version)
Additional Information	There are other files related to this item in HUSCAP. Check the above URL.
File Information	manuscript_revise_HCOOH_CO2_151205_af.pdf

Instructions for use

Selective synthesis of carbon monoxide via formates in reverse water-gas shift reaction over alumina-supported gold catalyst

Nobuhiro Ishito[a,b], Kenji Hara[a,c], Kiyotaka Nakajima[a,b], Atsushi Fukuoka[a,b,*]

[a] *Institute for Catalysis, Hokkaido University, Sapporo 001-0021, Hokkaido, Japan*

[b] *Graduate School of Chemical Sciences and Engineering, Hokkaido University, Sapporo 060-8628,*

Hokkaido, Japan

[c] *School of Engineering, Tokyo University of Technology, Hachioji 192-0982, Tokyo, Japan*

Abstract

Thermal decomposition of formic acid on SiO_2, CeO_2 and $\gamma\text{-}Al_2O_3$ was studied as an elementary step of reverse water-gas shit reaction (RWGS) over supported Au catalysts. $\gamma\text{-}Al_2O_3$ showed the highest CO selectivity among the tested oxides in the decomposition of formic acid. Infrared spectroscopy showed the formation of four formate species on $\gamma\text{-}Al_2O_3$: three η^1–type and one μ^2-type species, and these formates decomposed to CO at 473 K or higher. Au-loaded $\gamma\text{-}Al_2O_3$ samples were prepared by a deposition-precipitation method and used as catalysts for RWGS. The supported Au catalyst gave CO with high selectivity over 99% from CO_2 and H_2, which is attributed to the formation of formates on Au and subsequent decomposition to CO on $\gamma\text{-}Al_2O_3$.

Key words: Reverse water-gas shift reaction, Carbon dioxide, Hydrogen, Formate, Carbon monoxide, Alumina, Gold

* Corresponding author. Tel: +81-11-706-9140; Fax: +81-11-706-9139; E-mail: fukuoka@cat.hokudai.ac.jp

1. Introduction

Carbon dioxide (CO_2) has been recognized as an abundant and inexpensive carbon resource for chemical industry [1-4]. Reverse water-gas shift reaction (RWGS, equation 1) is one of the most important reactions in C1 chemistry, because the resulting carbon monoxide (CO) [5-9] can be utilized as feedstock for the production of valuable compounds such as methanol, dimethyl ether and hydrocarbons [5,8]. $Cu/ZnO/Al_2O_3$ is known as an active catalyst for RWGS and methanol synthesis from syngas (CO/H_2), and methanol can be directly obtained from CO_2 and H_2 [5,10-12]. Methanol synthesis from CO_2 and H_2 has been currently tested in a pilot plant with a cupper-based catalyst [13]. In contrast to the direct synthesis of methanol, the production of syngas from CO_2 is one of the key technologies for sustainable chemical production, because syngas can be converted to a variety of useful compounds in the Fischer-Tropsch synthesis [5,8,14,15].

$$CO_2 + H_2 \rightleftarrows CO + H_2O \tag{1}$$

Gold (Au) nanoparticles supported on various oxides have been investigated by Haruta *et al*. for the hydrogenation of CO_2 [16]. CO is a main product in this system, because the Au catalysts cannot catalyze CO hydrogenation to CH_4 or CH_3OH. Moreover, CO_2 conversion and product selectivity greatly depend on the acid-base property of the oxide supports. Au catalysts on acidic supports produce CO and a small amount of CH_4. On the other hand, Au catalysts on basic supports give low CO_2 conversion due to a strong interaction of CO_2 with basic sites.

It is known that formate species are formed as a key intermediate in the CO_2 hydrogenation over Au catalysts [5,17-20]. Since Au nanoparticles do not decompose the formate species [20,21], the decomposition of formate species is strongly influenced by the property of supports. In this work, we studied the decomposition of formate species on oxide supports such as SiO_2, γ-Al_2O_3 (hereafter Al_2O_3) and CeO_2 as an elementary step in RWGS over Au catalysts. Amphoteric Al_2O_3 converted formate species into CO with higher selectivity than SiO_2 and CeO_2. Thermal decomposition of formates on Al_2O_3 was evaluated by diffusive reflectance infrared Fourier transform spectroscopy (DRIFT). Then, Au-loaded Al_2O_3 samples were prepared and their catalytic activity was tested in RWGS.

2. Experimental

2.1. Reagents

Al_2O_3 was purchased from Tokyo Chemical Industry Company (Japan). Formic acid, $HAuCl_4 \cdot 3H_2O$ and diethyl ether with highest grade were obtained from Wako Pure Chemical Industries (Japan) and used without any purification treatment.

2.2. Thermal decomposition of formate species on metal oxides

Formic acid was immobilized on metal oxides (CeO_2, SiO_2, and Al_2O_3) by simple adsorption treatment. Each metal oxide (1.0 g) was added to a mixture of formic acid (1 mL) and diethyl ether (25 mL), and the solution was stirred at room temperature for 6 h under air. After filtration, the resulting materials were washed repeatedly with diethyl ether, and then dried under vacuum for 12 h. The amount of formic acid on each metal oxide was estimated by a total organic carbon analyzer (TOC, Shimadzu SSM-5000A). The samples were heated in an IR cell from 298 to 773 K with a heating rate of 2 K min^{-1} under a mixed gas flow of Ar (2 mL min^{-1}) and He (18 mL min^{-1}). The outlet gas was analyzed by gas chromatography (Shimadzu GC 8A, thermal conductivity detector, active carbon column (2 m), temperature 383 K) to monitor the evolved CO and CO_2. FT-IR spectra were obtained at a resolution of 1 cm^{-1} using a spectrometer (Spectrum 100, PerkinElmer) equipped with a mercury cadmium telluride (MCT) detector. A total of 16 scans were averaged for each spectrum. Deconvolution of peaks was performed by assuming Gaussian profiles of the peaks.

2.3. Catalyst preparation and catalytic reaction

An Au-loaded Al_2O_3 sample was prepared by a deposition-precipitation (DP) method [22]. Al_2O_3 was immersed in an aqueous solution of $HAuCl_4$ (pH 8), which was aged for 1 h. The resulting solid was filtered, washed with H_2O, dried at 383 K and reduced in H_2 at 573 K for 3 h to afford Al_2O_3-supported Au catalyst (denoted Au-DP). For comparison, an Al_2O_3-supported Au catalyst (Au 5 wt%) was prepared by a conventional impregnation method using $HAuCl_4 \cdot 3H_2O$ (99.9%, Wako). After immobilization of Au species on Al_2O_3 by vacuum evaporation and drying at 298 K, the sample was reduced in H_2 at 573 K for 3 h to obtain Al_2O_3-supported Au catalyst (denoted Au-Imp). Structural characterization of the catalysts was performed by X-ray fluorescence spectroscopy (XRF, EDX-720, Shimadzu), nitrogen adsorption (Belsorp-mini II, MicrotracBEL), X-ray diffraction (XRD, Rigaku, Ultima IV, Cu Kα) and transmission electron microscopy (TEM, JEM-2100F, JEOL, 200 kV).

Hydrogenation of CO_2 was conducted in a fixed-bed flow reactor (inner diameter 9.5 mm) made of SUS316 (Figure S1). Mass flows of CO_2 (99.95%), H_2 (99.999%), He (99.999%) and Ar (99.999 %, internal standard) were regulated by mass flow controllers (HORIBA STEC). The catalyst (0.3 g) was diluted with glass beads (diameter 0.2 mm, 1 g) and charged in the reactor. After reduction of the catalyst in H_2 flow (20 mL min^{-1}) at 673 K for 1 h and subsequent treatment in He flow (20 mL min^{-1}) at 673 K for 15 min, a gas mixture (CO_2 15 %, H_2 75%, Ar 10 %, flow rate 20 mL min^{-1}, space velocity (SV) 4,000 mL g^{-1} h^{-1}, 0.1 MPa) was fed into the reactor. Products in the liquid phase collected by a water-trap were analyzed by high-performance liquid chromatography (HPLC, Shimadzu LC10ATVP, UV detector) with a Shodex Sugar SH-1011 column (ø8×300 mm, eluent: water 0.5 mL min^{-1}, 323 K). The outlet gas was analyzed by gas chromatography (Shimadzu GC 8A, thermal conductivity detector, active carbon column (2 m), temperature 383 K).

3. Results and discussion

3.1. Thermal decomposition of formic acid on metal oxides

Thermal decomposition of formic acid produces CO_2+H_2 or $CO+H_2O$ (equation 2). In the reaction from the left to the right (RWGS), formic acid (HCOOH) is assumed to be an intermediate and selective decomposition of HCOOH to CO is important. Hence, the effect of supports on the decomposition of HCOOH was studied.

$$CO_2 + H_2 \rightleftarrows HCOOH \rightleftarrows CO + H_2O \quad (2)$$

Here we used three metal oxides for the decomposition of HCOOH into CO to find the most appropriate support of Au for RWGS. Table 1 compares the amount of adsorbed HCOOH and CO/CO_2 ratio in the decomposition of HCOOH. Similar amounts of HCOOH adsorbed on metal oxides estimated by TOC. However, the densities of immobilized HCOOH for Al_2O_3 and CeO_2 are larger than that for SiO_2. This difference is attributed to weakly basic property of Al_2O_3 and CeO_2 to stabilize HCOOH by the formation of formate. Decomposition of adsorbed species was examined by heating these oxides from room temperature to 773 K under inert gas atmosphere. SiO_2 decomposed HCOOH into CO and CO_2 equally ($CO/CO_2 = 1$). CeO_2 and Al_2O_3 produced CO more favorably than CO_2, and Al_2O_3 gave the highest CO/CO_2 ratio among the three oxides. Figure 1 shows dependence of CO and CO_2 formation on reaction temperature over Al_2O_3. CO evolution starts at 473 K and rapidly increases up to 543 K. On the

basis of CO evolution, decomposition is completed below 673 K. From these results, decomposition of HCOOH on Al_2O_3 was monitored by IR at 483-683 K.

Table 1. Adsorption and thermal decomposition of formic acid on Al_2O_3, CeO_2 and SiO_2.

Oxide	Amount of adsorbed formic acid (mmol g^{-1})[a]	Surface area ($m^2 g^{-1}$)	Density of adsorbed formic acid (nm^{-2})	CO / CO_2 ratio[b]
Al_2O_3	1.3	160	4.9	50
CeO_2	1.0	130	4.6	3
SiO_2	0.8	290	1.7	1

[a] Determined by TOC analysis, [b] CO and CO_2 were analyzed by GC-TCD.
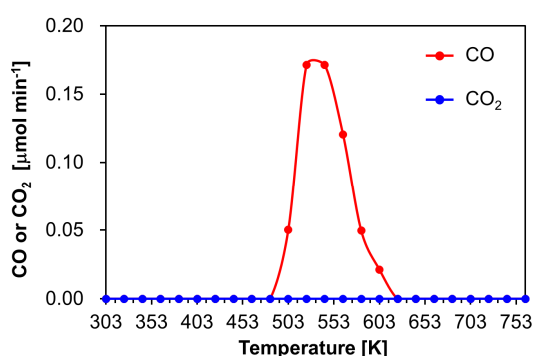
Figure 1. Dependence of CO (red) and CO_2 (blue) formation on reaction temperature over Al_2O_3.
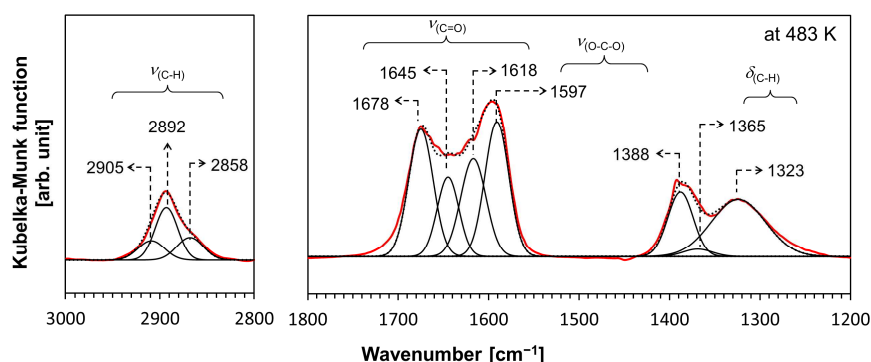

Figure 2. DRIFT spectrum of HCOOH-adsorbed Al_2O_3 at 483 K under inert gas atmosphere. Red line: raw spectrum, black dot line: combined spectrum of deconvoluted peaks.

Figure 2 shows a DRIFT spectrum of HCOOH-adsorbed Al_2O_3 at 483 K under inert gas atmosphere.

Broad bands at 3000-2800 cm^{-1}, 1800-1400 cm^{-1} and 1400-1200 cm^{-1} are assignable to C-H stretching, C-O stretching and C-H bending modes of adsorbed formic acid, respectively. Tamaru *et al.* reported that a formate species with η^1-type structure is an intermediate in the thermal decomposition of HCOOH on γ-Al$_2$O$_3$ (Figure 3a) [23]. Hence, the bands at 2892, 1678, 1323 cm^{-1} in Figure 2 are assignable to $\nu_{(C-H)}$, $\nu_{(C=O)}$ and $\delta_{(C-H)}$ of the η^1-type formate species. He *et al.* studied stretching vibration modes of the adsorbed formate species on Al$_2$O$_3$ by density functional theory (DFT) calculation and proposed that formate species in the form of μ^2-type structure can be stabilized (Figure 3c) [24]. Formation of the μ^2-type formate on Al$_2$O$_3$ was also confirmed from the IR bands at 2905 cm^{-1} ($\nu_{(C-H)}$), 1597 cm^{-1} ($\nu_{as(O-C-O)}$) and 1388 cm^{-1} ($\nu_{s(O-C-O)}$) in Figure 2. In addition to the bands for the typical η^1- and μ^2-type formates, four IR bands at 2858, 1645, 1618 and 1365 cm^{-1} are observed in Figure 2. The presence of two bands at 1645 and 1618 in the region of C=O stretching suggests that two different formate species other than η^1- and μ^2-type species are formed on Al$_2$O$_3$. Because the coordination of carbonyl group with Lewis acid sites results in red shift of original C=O stretching frequency, these bands are ascribed to η^1-type formates with carbonyl groups weakly interacting with an adjacent Lewis acid site (Figure 3b). It was reported that Al$_2$O$_3$ has three Lewis acid sites in terms of acid strength: strong, medium and weak Lewis acid sites [25]. The μ^2 species could be formed on the two strong Lewis acid sites, so that the bands at 1645 and 1618 cm^{-1} can be reasonably assigned to η^1 species interacting with weak and medium Lewis acid sites. The bands at 2858 and 1365 cm^{-1} in Figure 2 are assignable to $\nu_{(C-H)}$ and $\delta_{(C-H)}$ of these formate species. These three η^1 type formates are denoted η^1(1678 cm^{-1}), η^1(1645 cm^{-1}) and η^1(1618 cm^{-1}).

(a)   (b)   (c)

η^1 ($\nu_{(C=O)}$; 1678 cm^{-1}) η^1 ($\nu_{(C=O)}$; 1645 cm^{-1}) μ^2 ($\nu_{(O-C-O)}$; 1597, 1388 cm^{-1})
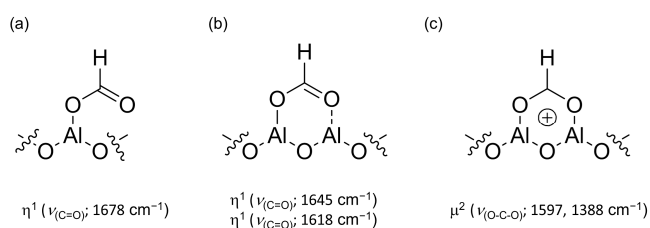η^1 ($\nu_{(C=O)}$; 1618 cm^{-1})

Figure 3. Proposed structures of adsorbed formate species on Al$_2$O$_3$: (a) typical η^1–type species, (b) two η^1–type species interacting with weak and medium Lewis acid sites and (c) typical μ^2–type species.

Decomposition of these formate species was evaluated by temperature-programmed DRIFT measurement (Figure S2). Figure 4a shows DRIFT spectra of HCOOH-adsorbed Al$_2$O$_3$ heated at

different temperatures. Specific bands for η^1(1678 cm^{-1}), η^1(1645 cm^{-1}), η^1(1618 cm^{-1}) and μ^2 species in 1800-1500 cm^{-1} changed continuously during the thermal treatment. The band intensities of the four formate species were plotted against each temperature (Figure 4b). It is clearly shown that the decrease in band intensity for the three η^1 species is well correlated with the increase in CO formation, which indicates that CO formation occurs by the decomposition of the η^1 species. In contrast, the μ^2 species shows higher thermal stability; most μ^2 species remains at ca. 573 K. Therefore, CO formation at higher temperature is mainly due to the decomposition of the μ^2 species.
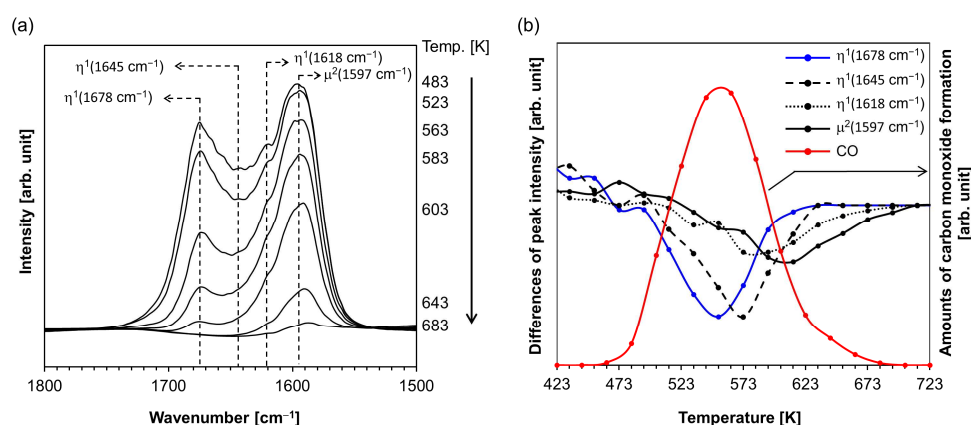

Figure 4. (a) DRIFT spectra of HCOOH-adsorbed Al$_2$O$_3$ at different temperatures and (b) temperature dependence of CO formation and band intensities for four formates.

3.2. Hydrogenation of carbon dioxide over alumina supported gold catalyst

As described in the previous section, formate species formed in adsorption of HCOOH on Al$_2$O$_3$ are readily decomposed to CO at above 483 K; therefore, it is expected that the introduction of Au nanoparticles on Al$_2$O$_3$ gives CO via HCOOH from CO$_2$ and H$_2$ [16]. Al$_2$O$_3$-supported Au catalysts were prepared by a deposition-precipitation (DP) method and an impregnation method (Imp). Figure 5 shows XRD patterns of the resulting catalysts. Several sharp or broad diffractions are observed for Al$_2$O$_3$, and all the diffractions are assignable to γ-phase of crystalline Al$_2$O$_3$. In addition to the peaks, Au-Imp showed five sharp diffractions at $2\theta = 38°$, 44°, 65°, 78° and 82° due to (111), (200), (220), (311) and (222) planes for face-centered cubic (FCC) lattice structure of Au metal [26]. An average size of Au

7

particles in Au-Imp was estimated to be 38 nm by the Scherrer equation. In contrast, Au-DP represented no diffractions of Au metal, which implies high dispersion of Au particles on the Al_2O_3 surface.
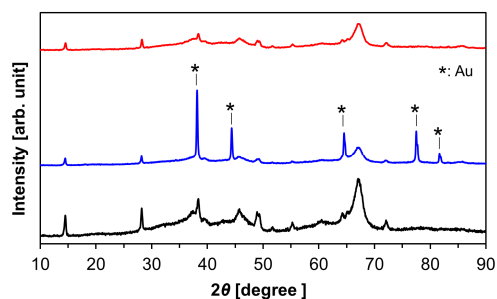

Figure 5. XRD patterns of γ-Al_2O_3 (black), Au-Imp (blue) and Au-DP (red).

Figure 6 is a TEM image of Au-DP, which reveals the presence of Au nanoparticles with a mean diameter of 2.6 nm. Thus, the DP method is appropriate for the preparation of Al_2O_3-supported Au catalyst.
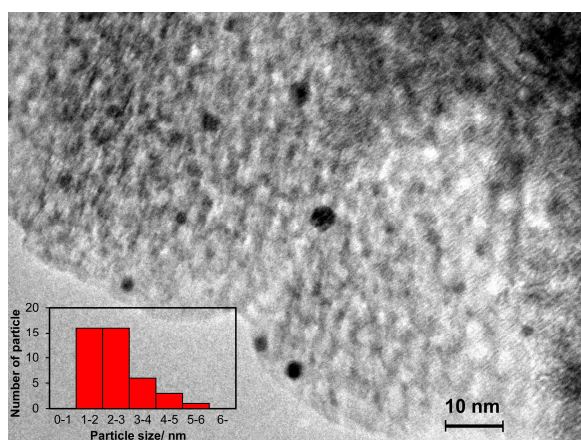

Figure 6. TEM image of Au-DP and size distribution of Au nanoparticles (inset).

RWGS was conducted at 623 K and 1 atm with a gas hourly space velocity (GHSV) of 4000 mL g^{-1} h^{-1}. A control experiment in the absence of catalyst gave no reaction (Table 2, entry 1). Au-Imp showed a very low CO_2 conversion (2.0%) (entry 2), but Au-DP gave 20% CO_2 conversion with high CO selectivity over 99% (entry 3). Accordingly, Au nanoparticles on Al_2O_3 can quantitatively produce CO even under atmospheric pressure. CO_2 equilibrium conversion is estimated to be ca. 38% under the reaction conditions by chemical thermodynamic parameters [27].

Table 2. Reverse water-gas shift reaction by Al_2O_3-supported Au catalysts[a]

Entry	Catalyst	Conversion (%)	CO yield (%)	CO selectivity (%)
1	None	0.0	0.0	0.0
2	Au-Imp	2.0	2.0	> 99
3	Au-DP	20	20	> 99

[a] Reaction condition: catalyst (50 mg), CO_2 (15%), H_2 (75%), Ar (10%), 623 K, 1 atm. Sampling after 30 and 45 min. Steady state was confirmed after 30 min.

Probably, such a high selectivity can be derived from the formation of formate species by Au nanoparticle and the subsequent decomposition to CO by Al_2O_3. The formation of formate species on Au/Al_2O_3 catalyst was directly confirmed by DRIFT measurement. Figure 7 shows DRIFT spectra of Au-DP at 473 K under a flow of CO_2 and H_2. After reduction of the catalyst in H_2 flow (20 mL min^{-1}) at 673 K for 1 h and subsequent treatment in He flow (20 mL min^{-1}) at 673 K for 15 min, a gas mixture (CO_2 15 %, H_2 75%, Ar 10 %, flow rate 20 mL min^{-1} 0.1 MPa) was continuously fed into the IR cell during the measurement. One intense and asymmetric band is observed at 1597 cm^{-1}. Heat treatment at 473 K enables efficient removal of physisorbed water formed by the RWGS reaction, so that the band is regarded as a combined band for η^1(1678 cm^{-1}), η^1(1645 cm^{-1}), η^1(1618 cm^{-1}) and μ^2 (1597 cm^{-1}) species of adsorbed formate on Al_2O_3 (Figure 4a). Due to low thermal stability for η^1(1678 cm^{-1}), η^1(1645 cm^{-1}), and η^1(1618 cm^{-1}), the bands started to decrease gradually in their intensities from 473 K, while the band for μ^2 (1597 cm^{-1}) species retained intact even at 623 K. This tendency was good agreement with the result for thermal decomposition of adsorbed HCOOH on Al_2O_3 (Figure 4b). Moreover, Au nanoparticles cannot adsorb and decompose formate species [21], which means that they are formed by Au nanoparticle and stabilized on Al_2O_3 support before subsequent decomposition into CO and H_2O. Au-DP is therefore an effective catalyst for selective formation of CO from a mixture of CO_2 and H_2.
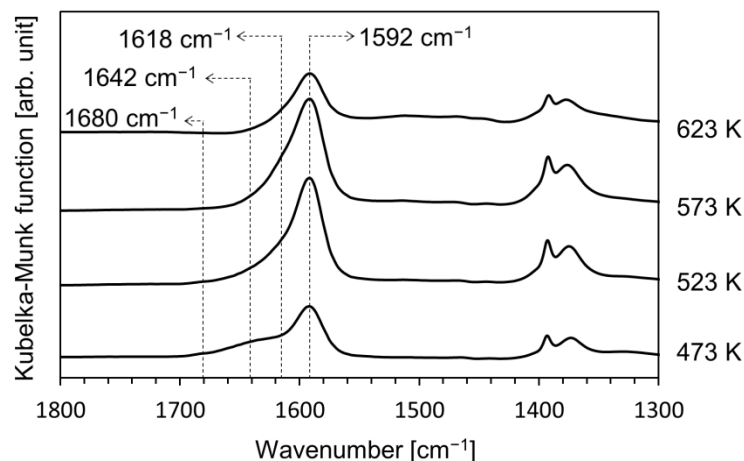
Figure 7. DRIFT spectra of Au-DP at different temperatures under a gas flow of H_2 and CO_2.

4. Conclusions

HCOOH adsorbed on Al_2O_3 selectively decomposed to CO. The decomposition pathway on Al_2O_3 was monitored by in-situ FTIR measurement, and four types of formate species were observed on Al_2O_3. Three η^1-type formates were well correlated with the formation of CO, but one μ^2-type formate was thermally stable and decomposed to CO at higher temperature. Selective decomposition of formates to CO is a great advantage of Al_2O_3 as a support of Au. Al_2O_3-supported Au catalyst was prepared by a deposition-precipitation method, and this catalyst gave CO with high selectivity (> 99%).
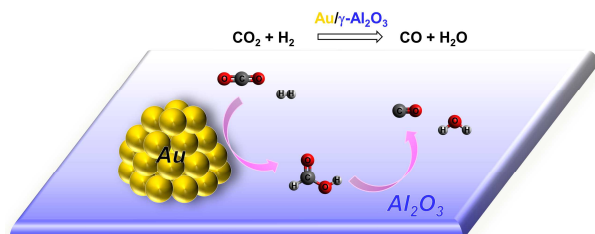
References:

[1] G. Centi, S. Perathoner, Catalysis Today 148 (2009) 191.

[2] T. Schaub, R. A. Paciello, Angew. Chem. Int. Ed. 50 (2011) 7278.

[3] S. Fukuoka, M. Kawamura, K. Komiya, M. Tojo, H. Hachiya, K. Hasegawa, M. Aminaka, H. Okamoto, I. Fukawa, S. Konno, Green Chem. 5 (2003) 497.

[4] G. W. Coates, D. R. Moore, Angew. Chem. Int. Ed. 43 (2004) 6618.

[5] W. Wang, S. Wan, X. Ma, J. Gong, Chem. Soc. Rev. 40 (2011) 3703.

[6] R. Tanaka, M. Yamashita, K. Nozaki, J. Am. Chem. Soc. 131 (2009) 14168.

[7] J. Sloczynski, R. Grabowski, A. Kozlowka, P. Olszewski, J. Stoch, J. Skrzypek, M. Lachowska, Appl. Catal. A 278 (2004) 11.

[8] R. W. Dorner, D. R. Hardy, F. W. Williams, H. D. Willauer, Appl. Catal. A 373 (2010) 112.

[9] O. S. Joo, K. D. Jung, I. Moon, A.Y. Rozovskii, G.I. Lin, S. H. Han and S. J. Uhm, Ind. Eng. Chem. Res. 38 (1999) 1808.

[10] F. S. Stone, D. Waller, Topics in catalysis 22 (2003) 305.

[11] Y. Zhang, Q. Sun, J. Deng, D. Wu, S. Chen, Appl. Catal. A 158 (1997) 105.

[12] M. Behrens, F. Studt, I. Kasatkin, S. Kühl, M. Hävecker, F. Abild-Pedersen, S. Zander, F. Girgsdies, P. Kurr, B. L. Kniep, M. Tovar, R. W. Fischer, J. K. Nørskov, R. Schlögl, Science 336 (2012) 893.

[13] T. Matsushita, T. Haganuma, D. Fujita US Patent 20130237618, 2013.

[14] G. Kiss, M. G. Matturro, H. W. Deckman, F. Hershkowitz, D. R. Lumgir, G. F. Janda, D. N. King US Patent 6049011, 2000.

[15] P. Liu, E. N. Jacobsen, J. Am. Chem. Soc. 123 (2001) 10772.

[16] H. Sakurai, S. Tsubota, M. Haruta, Appl. Catal. A 102 (1993) 125.

[17] G. Jacobs, A. C. Crawford, B. H. Davis, Catal. Lett. 100 (2005) 147.

[18] Q. Y. Bi, X. L. Du, Y. M. Liu, Y. Cao, H. Y. He, K. N. Fan, J. Am. Chem. Soc. 134 (2012) 8926.

[19] R. A. Koeppel, A. Baiker, C. Schild, A. Wokaun, J. Chem. Soc. Faraday Trans. 87 (1991) 2821.

[20] D. Preti, C. Resta, S. Squarcialupi, G. Fachinetti, Angew. Chem. Int. Ed. 50 (2011) 12551.

[21] W. J. M. Rootsaert, W. M. H. Sachtler, J. Phys. Chem. 26 (1960) 16.

[22] M. Haruta, Catalysis Today 36 (1997) 153.

[23] Y. Noto, K. Fukuda, T. Onishi, K. Tamaru, Trans. Faraday Soc. 63 (1967) 2300.

[24] H. Gao, T. Yan, C. Zhang, H. He, THEOCHEM 857 (2008) 38.

[25] X.Liu, R. E. Truitt, J. Am. Chem. Soc. 119 (1997) 9856.

[26] Y. Shao, Y. Jin, S. Dong, Chem. Commun. (2004) 1104.

[27] D. D. Wagman, W. H. Evans, V. B. Parker, R. H. Schumm, I. Halow, S. M. Bailey, K. L. Churney, R. L. Nuttall, J. Phys. Chem. Ref. Data Vol.11, supplement No.2 (1982).

Description portion (20-30 words)

Selective formation of carbon monoxide in reverse water-gas shift reaction by way of thermal decomposition of formic acid as an intermediate over alumina-supported gold catalyst (25 words)

Graphic abstract (50 mm high × 85 mm wide)

(32.65 mm high×78.85 mm wide)